Thermal fission rates with temperature dependent fission barriers

Yi Zhu (朱怡) and J. C. Pei (裴俊琛)*
State Key Laboratory of Nuclear Physics and Technology, School of Physics, Peking University, Beijing 100871, China
(Received 15 May 2016; published 19 August 2016)

Background: The fission processes of thermal excited nuclei are conventionally studied by statistical models which rely on inputs of phenomenological level densities and potential barriers. Therefore the microscopic descriptions of spontaneous fission and induced fission are very desirable for a unified understanding of various fission processes.
Purpose: We propose to study the fission rates, at both low and high temperatures, with microscopically calculated temperature-dependent fission barriers and collective mass parameters.
Methods: The fission barriers are calculated by the finite-temperature Skyrme-Hartree-Fock+BCS method. The mass parameters are calculated by the temperature-dependent cranking approximation. The thermal fission rates can be obtained by the imaginary free energy approach at all temperatures, in which fission barriers are naturally temperature dependent. The fission at low temperatures can be described mainly as a barrier-tunneling process. While the fission at high temperatures has to incorporate the reflection above barriers.
Results: Our results of spontaneous fission rates reasonably agree with other studies and experiments. The temperature dependencies of fission barrier heights and curvatures have been discussed. The temperature dependent behaviors of mass parameters have also been discussed. The thermal fission rates from low to high temperatures with a smooth connection have been given by different approaches.
Conclusions: Since the temperature dependencies of fission barrier heights and curvatures, and the mass parameters can vary rapidly for different nuclei, the microscopic descriptions of thermal fission rates are very valuable. Our studies without free parameters provide a consistent picture to study various fissions such as that in fast-neutron reactors, astrophysical environments, and fusion reactions for superheavy nuclei.

DOI: 10.1103/PhysRevC.94.024329

I. INTRODUCTION

The microscopic description of the fission process as a large amplitude collective motion is one of the well-known challenges in nuclear many-body theory, and still large uncertainties exist towards a predictive theory of fission [1,2]. Basically, the spontaneous fission can be described as quantum tunneling based on potential barriers and collective mass parameters, which can be microscopically calculated by nuclear energy density functional theory. In this respect, there are a number of approaches to describe the collective mass such as the cranking approximation [3], the generate-coordinate method (GCM) [4], the adiabatic-time-dependent Hartree-Fock-Bogoliubov approach (ATDHFB) [3], and the local QRPA method [5]. For fission barriers, there are also many efforts either to improve descriptions of potential energy surfaces at large deformations [6] or to seek multidimensional constrained calculations [7–9].

In addition to issues involved in spontaneous fission, the description of thermal fission in excited nuclei is a more demanding task. From low to high temperatures, the fission process is gradually evolved from the quantum tunneling to the statistical escape mechanism. For applications, the thermal fission has a wide range of interests such as the neutron induced fission in reactors and in astrophysical environments, and fusion reactions for superheavy nuclei. Conventionally, the thermal fission is described by the Bohr-Wheeler transition-state theory and later the dynamical Kramers theory [10]. The imaginary free energy approach (ImF) is a general thermodynamic method to calculate thermal quantum decay rates at all temperatures [11,12], which has been widely applied to decays of metastable states such as nuclear fissions [13] and chemical reactions [14]. These methods rely on inputs of barriers or level densities, which are dependent on temperatures, deformations, and shell structures. As a consequence, many corrections and associated parameters have been introduced to interpret experimental results. Therefore, a consistent description of thermal fission with microscopic inputs that are free of parameters, from low to high temperatures, is very desirable.

In a microscopic view, the thermal excited nuclei can be described by the finite-temperature Hartree-Fock-Bogoliubov (FT-HFB) theory (or FT-HF+BCS) [15]. In FT-HFB, the thermal excitations of compound nuclei are described as quasiparticle excitations due to a finite temperature in a heat bath. The quantum effects: the superfluidity and shell effects, would self-consistently fade away with increasing temperatures [16]. The fission barriers can be either isothermal or isentropic in terms of free energies [17]. In previous works [17–19], we have studied the neutron emission rates and fission barriers in compound superheavy nuclei microscopically. We feel an obligation to study further the thermal fission rates with the temperature dependent fission barriers.

In the Kramers and ImF methods, the fission barriers are in terms of free energies which are naturally temperature dependent [10,12]. It has been realized that the temperature dependent fission barrier should be considered in fission calculations [20]. It is turned out that the Bohr-Wheeler fission calculations also have to introduce damping factors to describe the decreasing fission barriers with

*peij@pku.edu.cn

increasing excitation energies to interpret survival probabilities of compound nuclei [21,22]. We have demonstrated that the temperature dependence of fission barriers can vary rapidly for specific nuclei [17,23], indicating non-negligible shell effects in hot-fusion reactions. This has attracted much attention from experimentalists [24,25]. Further, the temperature dependent fission barriers in two-dimensional deformation spaces have been studied [26], showing the fission modes become symmetric at high temperatures. In addition to the fission barrier heights, the curvatures around the equilibrium point and the saddle point can also be dependent on temperatures, which are essential inputs for Kramers and ImF methods. This can also be microscopically described but has rarely been discussed.

Another essential ingredient for describing thermal fission is the temperature dependent mass parameter. This has been studied by several phenomenological mean-field methods with the finite-temperature cranking approximation [27,28]. It is difficult to consider the temperature dependence in GCM and ATDHFB calculations of mass parameters. There has also been microscopic studies with Gogny forces for the temperature dependent cranking mass parameters [29]. In fact, the temperature dependent mass parameters have not yet been incorporated into serious calculations of thermal fission rates.

In this work, we intend to study the thermal fission rates with microscopically calculated temperature dependent fission barriers and mass parameters. The calculations are based on the finite-temperature Skyrme Hartree-Fock+BCS framework in deformed coordinate spaces including octupole deformations. The coordinate-space calculations can naturally describe very elongated nuclear shapes. The mass parameters are calculated with the cranking approximation with temperatures. The thermal fission rates in principle can be described consistently by the ImF method from low to high temperatures. At low temperatures, the quantum tunneling process is dominated and the WKB method is adopted. At high temperatures, the semiclassical reflection process above barriers is considered [30]. With microscopic inputs of potential barriers and mass parameters, we will see that the thermal fission from low to high temperatures can be described in a consistent picture.

Presently our studies are restricted to one-dimensional fission although both quadrupole and octupole deformations are included. Indeed, the multidimensional fission descriptions are more realistic and computationally more costly. In the semiclassical approximation, a multidimensional tunneling problem can be transformed into an effective one-dimensional problem [14]. Thus the one-dimensional thermal fission has already involved essential issues in the multidimensional fission. Besides, we have not considered the viscosity and dissipations which are important at high temperatures. Thus our studies are limited to a moderate temperature of $T =$ 1.5 MeV that has already included the hot-fusion reactions for superheavy nuclei. For realistic nonadiabatic descriptions, it is known that the real-time-dependent density functional theory for fission dynamics is only applicable after saddle points [31–34], which are useful for studying fission fragment distributions. In this case the semiclassical descriptions of the thermal fission process with microscopic inputs are promising for multidimensional problems [35]. The present paper can be seen as a basic theoretical attempt towards fully microscopic descriptions of the thermal fission, instead of the conventional statistical models.

II. THEORETICAL FRAMEWORK

In this section we will discuss the theoretical methods to calculate the spontaneous fission rates, the temperature dependent fission barriers and mass parameters, and the thermal fission rates. The thermal fission rates from low to high temperatures are given by the ImF method.

A. Spontaneous fission rates

The spontaneous fission rates can be evaluated by the WKB method as a quantum tunneling process along fission pathways [36,37]. The fission path is obtained by the constrained Skyrme-Hartree-Fock+BCS calculations in the axially symmetric coordinate-space, including the reflection asymmetry. The Skyrme-Hartree-Fock+BCS equation is solved by the SKYAX solver [38]. In our calculations, the Skyrme interaction SkM* [39] and the mixed pairing interaction [40] have been adopted. The SkM* parameter set has been optimized by including fission barrier heights and has been widely used for microscopic fission studies. The pairing strengthes are taken as $V_p = 522$ and $V_n = 435$ MeV fm^{-3} by fitting the pairing gaps of ^{252}Fm.

The fission width Γ along the fission pathway s can be calculated by $\Gamma = P/F$ as [36]

$$P = \left[1 + \exp\left(2\int_b^c \sqrt{2M(s)(V(s) - E_0)}ds\right)\right]^{-1}, \quad \text{(1a)}$$

$$F = \int_a^b ds \left(\sqrt{\frac{(E_0 - V(s)}{2M(s)}}\right)^{-1}, \quad \text{(1b)}$$

where the tunneling energy E_0, tunneling points a, b, and c are illustrated in Fig. 1. The potential energy surface $V(s)$ is given by Skyrme-Hartree-Fock+BCS calculations of binding

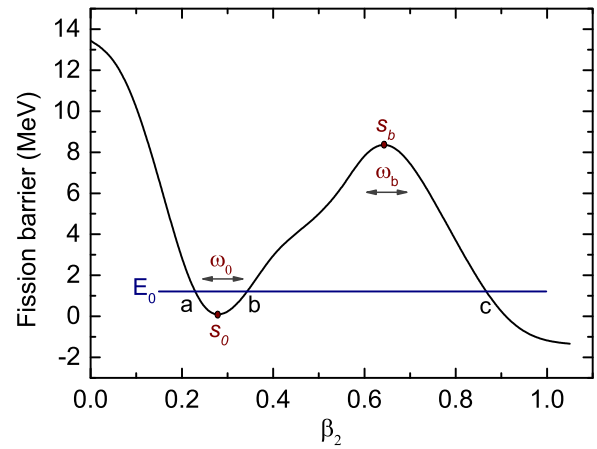

FIG. 1. The fission barrier of ^{260}Fm is shown to illustrate calculations of fission processes with a decay energy E_0. The potential frequencies (or curvatures) around the equilibrium point s_0 and the saddle point s_b are labeled as ω_0 and ω_b, respectively.

energies. The collective mass parameter $M(s)$ is given by the cranking approximation. The fission lifetime is calculated by $\hbar/\Gamma$. In Eq. (1), P is the penetration probability and F is an approximate normalization factor before tunneling, which is similar to the α-decay formula [41]. The normalization factor is actually related to the assaulting rate, which has been approximately taken as $10^{20.38}$ per second in Refs. [27,37].

To explain the normalization factor, we assume the potential valley can be described as a one-dimensional harmonic oscillator potential $\frac{1}{2}M\omega_0^2 s^2$, then we have

$$F = \int_a^b ds \left(\sqrt{\frac{E - \frac{1}{2}M\omega_0^2 s^2}{2M}} \right)^{-1} = \frac{2\pi}{\omega_0} \tag{2}$$

which demonstrated that $1/F$ is related to the assaulting frequency $\omega_0/2\pi$ on the fission barriers, irrespective of the decay energies. With the assumption of a harmonic potential, the decay energy E_0 and $\frac{1}{2}\hbar\omega_0$ (the collective ground state energy) should be equivalent. The assaulting rate of $10^{20.38}$ per second is related to $E_0 = 0.5$ MeV and $\hbar\omega_0 = 1$ MeV. Note that the calculated fission lifetimes are sensitive to E_0 and it is still an issue to determine E_0 in the literature. An assumption of E_0 as $0.7E_{\rm zpe}$ (the zero-point energy) was successful to reproduce the experimental results [37]. For realistic potentials, we can also estimate E_0 by the quantization condition [42]. For simplicity, our calculations are restricted to one-dimensional barriers, i.e., the fission path (including octupole deformations) is a function of quadrupole deformation β_{20}. It should be more realistic to estimate the collective ground state energy E_0 with other degrees of freedom in multidimensional cases for complex fission pathways.

We calculate the collective mass parameters microscopically for the WKB calculations of spontaneous fission rates. Based on Skyrme-Hartree-Fock+BCS calculations, the mass parameter $M_{20}(s)$ is calculated by the perturbative cranking approximation as [3]

$$M_{20} = \hbar^2[\mathcal{M}^{(1)}]^{-1}[\mathcal{M}^{(3)}][\mathcal{M}^{(1)}]^{-1}, \tag{3a}$$

$$\mathcal{M}_{ij}^{(K)} = \frac{1}{2}\sum \frac{\langle 0|Q_i|\mu\nu\rangle\langle\mu\nu|Q_j|0\rangle}{(E_\mu + E_\nu)^K}(u_\mu v_\nu + u_\nu v_\mu)^2, \tag{3b}$$

where v_μ^2 is the BCS occupation number; E_μ is the BCS quasiparticle energy. The perturbative cranking approximation of mass parameters can substantially overestimate the fission rates [7], compared to the nonperturbative cranking approximation, although the perturbative cranking approximation has been widely used [37].

B. Temperature dependent fission barriers

Our main objective in this work is to study the thermal fission rates with temperature dependent fission barriers. We have previously studied the thermal fission barriers of compound superheavy nuclei with the finite-temperature Hartree-Fock-Bogoliubov method [17,23]. In this work, based on the Skyrme-Hartree-Fock+BCS solver, we implement the finite-temperature BCS calculations according to Ref. [15]. With a given temperature T, the normal density ρ and the pairing density $\tilde{\rho}$ have to be modified as

$$\rho_T(\boldsymbol{r}) = \sum_i \left[v_i^2(1-f_i) + u_i^2 f_i\right]|\phi_i(\boldsymbol{r})|^2$$
$$\tilde{\rho}_T(\boldsymbol{r}) = \sum_i u_i v_i(1-2f_i)|\phi_i(\boldsymbol{r})|^2, \tag{4}$$

where $f_i = 1/(1+e^{E_i/kT})$ is the temperature dependent distribution factor, E_i is the BCS quasiparticle energy, k is the Boltzmann constant. Other density functionals can also be modified similar to the normal density. The particle number conservation equation is modified as

$$N = 2\sum_{i>0}\left[v_i^2 + \left(u_i^2 - v_i^2\right)f_i\right]. \tag{5}$$

The entropy is obtained by

$$S = -k\sum_i [f_i \ln f_i + (1-f_i)\ln(1-f_i)]. \tag{6}$$

Finally the temperature dependent fission barriers are calculated in terms of the free energy $F = E(T) - TS$, where $E(T)$ is the intrinsic binding energy. The temperature dependence of fission barriers can be related to the melting down of shell effects and has been found to be important to explain the experimental survival probabilities [21]. In addition to barrier heights, the temperature dependencies of curvatures of the potential valley and the barrier are also essential inputs for fission calculations, which are natural results of microscopic calculations. In this work, the beyond mean-field corrections to potential barriers have not been included, which are important at the zero temperature [43]. The SkM* force [39] that includes fission barriers in the fitting procedure could partially consider such effects.

C. Temperature dependent mass parameters

The temperature dependent collective mass parameters can be obtained by the cranking approximation with temperatures. Compared to expressions at the zero temperature, the pairing occupation numbers have to be explicitly modified as [28,44]

$$\begin{aligned}\mathcal{M}_{ij,T}^{(K)} = {} & \frac{1}{2}\sum_{\mu\neq\nu}\langle 0|Q_i|\mu\nu\rangle\langle\mu\nu|Q_j|0\rangle \\ & \left\{\frac{(u_\mu u_\nu - v_\mu v_\nu)^2}{(E_\mu - E_\nu)^K}\left[\tanh\left(\frac{E_\mu}{2kT}\right) - \tanh\left(\frac{E_\nu}{2kT}\right)\right]\right\} \\ & + \frac{1}{2}\sum\langle 0|Q_i|\mu\nu\rangle\langle\mu\nu|Q_j|0\rangle \\ & \left\{\frac{(u_\mu v_\nu + u_\nu v_\mu)^2}{(E_\mu + E_\nu)^K}\left[\tanh\left(\frac{E_\mu}{2kT}\right) + \tanh\left(\frac{E_\nu}{2kT}\right)\right]\right\}.\end{aligned} \tag{7}$$

We add a smooth factor of 1.0 in the denominator to avoid numerical divergence when two quasiparticle energies are close. The behaviors of temperature dependent mass parameters have been studied in several earlier publications [28,29,44].

D. Thermal fission rates at low temperatures

The microscopic descriptions of fission process at low temperatures are very interesting to study the induced fission. The fission at low temperatures can basically be considered as a quantum tunneling process, based on the temperature dependent fission barriers and mass parameters. In contrast to the spontaneous fission, the thermal fission involves excited states which are distributed statistically in terms of excitation energies. The excited states with energies of E_n within the potential valley are quasistationary and can be approximately described by the Bohr-Sommerfeld quantization condition [42],

$$\int_a^b ds\sqrt{2M_T(s)[E_n - V_T(s)]} = (n + 1/2)\pi, \tag{8}$$

where V_T and M_T are temperature dependent potential barriers and mass parameters. For the spontaneous fission, we only consider the tunneling energy E_0. For the thermal fission, we need to consider all the eigenstates with E_n lower than barriers.

Based on the spontaneous fission formula, the average thermal fission width at a temperature T ($\beta = 1/kT$) is obtained straightforwardly with the Boltzmann distribution, and is written as

$$\Gamma(T) = \frac{\sum_n \exp(-\beta E_n)P(E_n)/F(E_n)}{\sum_n \exp(-\beta E_n)}, \tag{9a}$$

$$P(E_n) = \left[1 + \exp\left(2\int_b^c \sqrt{2M_T(s)(V_T(s) - E_n)}ds\right)\right]^{-1}, \tag{9b}$$

$$F(E_n) = \int_a^b ds\left(\sqrt{\frac{(E_n - V_T(s)}{2M_T(s)}}\right)^{-1}. \tag{9c}$$

In Eq. (9), the energies E_n of collective quasiboundary states within the potential valley are obtained from Eq. (8). Obviously, this formula is only suitable at very low temperatures since E_n are lower than barriers. In addition, Eq. (9) would be problematic if ω_0 is very large and the number of states within the potential valley is not sufficient.

For comparison, we like to introduce the imaginary free energy method [11,12,45] which is more strict. In this method the quantity of interest is the free energy of the metastable system. To obtain the imaginary part of the free energy, it is key to calculate the partition function as a functional integral over the contour [11]. The decay probability is related to the imaginary free energy. The ImF formula at low temperatures is given as [12]

$$\Gamma = \frac{1}{Z_0}\frac{1}{2\pi\hbar}\int_0^{V_b} P(E)\exp(-\beta E)dE,$$
$$Z_0 = \left[2\sinh\left(\frac{1}{2}\beta\hbar\omega_0\right)\right]^{-1}, \tag{10}$$

where ω_0 is the frequency around the equilibrium point of the potential valley; V_b is the barrier height; Z_0 is the partition function.

We see the expression Eq. (9) is similar to the ImF formula Eq. (10) but with an additional normalization factor F, or the assaulting frequency. We refer Eq. (9) as the low-temperature Boltzmann fission formula. The difference of the resulted lifetimes between Eqs. (9) and (10) is generally within a factor of 5. The Boltzmann fission formula can self-consistently consider the temperature dependence of the assaulting frequency. It has been discussed that a slowly changed temperature-dependent assaulting frequency should be more reasonable than the constant $(2\pi\hbar)^{-1}$ in the ImF theory [46].

Without dissipation, the estimated transition temperature from quantum tunnelings to thermal decays is related to ω_b by [12]

$$T_c = \frac{\hbar\omega_b}{2\pi k}. \tag{11}$$

For instance, T_c is 0.24 MeV with $\omega_b = 1.5$ MeV, which is a very low temperature. For realistic potentials, we see that the low temperature ImF formula can be applied to temperatures that are slightly higher than T_c when the above-barrier decay ratio is still small.

E. Thermal fission rates at high temperatures

The thermal fission rates of compound nuclei at high temperatures are of great interests for productions of superheavy nuclei. In particular, the ^{48}Ca-induced hot fusion experiments have been very successful [24]. In contrast to the fission at low temperatures that is mainly a quantum tunneling process, the thermal fission at high temperatures needs to consider the reflection above barriers.

For energies above barriers, the refection can be considered as a tunneling process in the momentum space [30], which is difficult to be evaluated for complex-shaped barriers. In a special case, the reflection above a parabolic potential can be analytically obtained. Therefore, we can approximate the temperature-dependent barrier by an inverted harmonic oscillator potential,

$$V_{\rm barrier}(s) = V_b - \tfrac{1}{2}M\omega_b^2(s - s_{\rm b})^2, \tag{12}$$

where V_b is the barrier height, M is the mass parameter at the saddle point s_b, and ω_b is the barrier curvature (or frequency).

It is crucial to estimate the fission potential valley frequency ω_0 and the barrier frequency ω_b. Usually the frequencies are given by the second-order derivative of the potential as

$$\omega_0 = \sqrt{\frac{V''(s_0)}{M(s_0)}}, \quad \omega_b = \sqrt{-\frac{V''(s_b)}{M(s_b)}}. \tag{13}$$

However, the microscopic mass parameters are very much dependent on the deformation coordinates, as shown in Sec. III. For realistic potential barriers and mass parameters, we can extract ω_0 and ω_b approximately by

$$\omega_0 = \pi E \Big/ \int_a^b \sqrt{2M_T(s)(E - V_T(s))}ds,$$
$$\omega_b = \pi(V_b - E) \Big/ \int_b^c \sqrt{2M_T(s)(V_T(s) - E)}ds \tag{14}$$

which is exact with a harmonic oscillator potential. In principle, results of Eqs. (13) and (14) should be close. It

is turned out that Eq. (14) is roughly independent of E and is more reliable by avoiding the uncertainties in searching of minimum and saddle points.

The decay rate with an energy E above the inverted harmonic oscillator potential is written as

$$\frac{1}{2\pi\hbar}\{1+\exp(-2\pi(E-V_b)/\hbar\omega_b)\}^{-1}. \quad (15)$$

According to the ImF method for temperatures higher than T_c, the averaged fission rate after integral over E is written as [12]

$$\Gamma = \frac{\omega_b}{2\pi}\frac{\sinh\left(\frac{1}{2}\beta\hbar\omega_0\right)}{\sin\left(\frac{1}{2}\beta\hbar\omega_b\right)}\exp(-\beta V_b), \quad (16)$$

which can be related to the Kramers formula at high temperatures [12]:

$$\Gamma_{\rm Kramers} = \frac{\omega_0}{2\pi}\exp(-\beta V_b). \quad (17)$$

The Bohr-Wheeler formula should be basically consistent with the Kramers formula without dissipation [47]. While the influences of barrier widths or ω_b has not been considered in the Bohr-Wheeler formula and the static Kramers formula, which are the special cases of the ImF method. Based on the ImF formula Eq. (16), we see that the fission lifetimes would be increased by decreasing frequencies ω_0 or ω_b at high temperatures.

In principle, the ImF method works for thermal quantum decays at all temperatures consistently. The thermal fission at high temperatures involving dissipations and dynamical effects is complicated and the ImF method has been extended to dissipative decays [13,45,46]. The formula of thermal fission rates also becomes complicated considering the deformation dependent mass parameters [48]. Nevertheless, the microscopic temperature-dependent ω_0, ω_b, and V_b can provide an opportunity to look for other absent influences.

III. RESULTS AND DISCUSSIONS

In this section we study the spontaneous fission rates and thermal fission rates of some interested nuclei: ^{240}Pu, ^{260}Fm, ^{278}Cn, and ^{292}Fl. ^{240}Pu has a very long fission lifetime and usually has been chosen for fission benchmark studies [2]. ^{260}Fm is also an ideal testing case having a single barrier and a primary symmetric fission mode [8]. ^{278}Cn and ^{292}Fl are typical cold-fusion and hot-fusion compound superheavy nuclei in experiments [24], respectively.

A. Spontaneous fission rates

Firstly we studied the spontaneous fission rates of selected nuclei: ^{240}Pu, ^{260}Fm, ^{278}Cn, ^{292}Fl, as shown in Table I. The calculations are based on the SkM* Skyrme force and the mixed pairing. It has been pointed out that the cranking mass should be increased to simulate the ATDHFB mass [42]. In this work, we adopt the cranking mass that is scaled by a factor of 1.3, as suggested in Ref. [42]. Then E_0 is obtained by using the quantization condition. For ^{240}Pu, we include the asymmetric fission path of ^{240}Pu which is important for reducing the second barrier height. The calculated lifetime is still much larger than the experimental result mainly due to the absence of nonaxial symmetry, which can reduce the first barrier height [49]. For ^{260}Fm, the calculated fission lifetime agree with that of similar calculations with SkM* in Ref. [37]. ^{292}Fl has a very long calculated fission lifetime with a small E_0, as discussed in the following subsection. Note that the first barrier and the fission lifetime of ^{292}Fl could also be reduced by the inclusion of triaxial deformations. Generally, our results agree with other studies that also adopted the SkM* force. Indeed, the theoretical lifetimes are expected to be reduced with multidimensional fission pathways [50].

TABLE I. The calculated spontaneous fission lifetimes (in seconds) of selected nuclei, in which E_0 is obtained by the quantization condition. The experimental data are also given for comparison.

Nuclei	Expt (s) [55]	T_{SF} (s)	E_0 (MeV)
^{240}Pu	3.6×10^{18}	2.73×10^{22}	0.92
^{260}Fm	5.8×10^{-3}	4.25×10^{-3}	0.65
^{278}Cn		6.39×10^{-5}	0.90
^{292}Fl		8.56×10^{4}	0.46

Note that the fission lifetimes are sensitive to the different approaches to estimate the decay energies E_0. In this work, E_0 is related to the potential frequency at the ground state by the Bohr-Sommerfeld quantization condition and is not a free parameter, as given in Table I. Since the potential valley is not a perfect harmonic potential, we keep in mind that the estimation of E_0 can have considerable uncertainties. For example, E_0 has to be 1.41 MeV to reproduce the fission lifetime of ^{240}Pu, which can reduce the lifetime by 4 orders of magnitude compared to $E_0 = 0.92$ MeV. For ^{292}Fl, the ground state is slightly oblate and has a very soft potential energy surface (shown in Fig. 3) and the resulted E_0 is very small, which can substantially increase the fission lifetime.

Figure 2 displays the calculated fission barriers and mass parameters of ^{260}Fm by three different Skyrme forces: SkM* [39], SLy6 [51], and UNEDF1 [6], respectively. The SkM* and UNEDF1 forces have been optimized by including fission barrier heights. SLy6 is suitable for large deformations and surface properties by considering self-consistent center-of-mass corrections [52]. One can see that fission barriers of SkM* and SLy6 calculations are close. On the other hand, the cranking mass parameters of SkM* and UNEDF1 calculations are close. We note that the small differences in barriers or mass parameters can remarkably affect the fission rates. Such dependencies can be reduced with minimum action fission pathways in multidimensional calculations [53]. The SkM* force has been widely used for spontaneous fission calculations and is adopted for studies of thermal fission rates in this work. In addition to the dependence of Skyrme forces, the spontaneous fission lifetimes can also be reduced significantly with enhanced pairing strengthes, as discussed in Refs. [7,54].

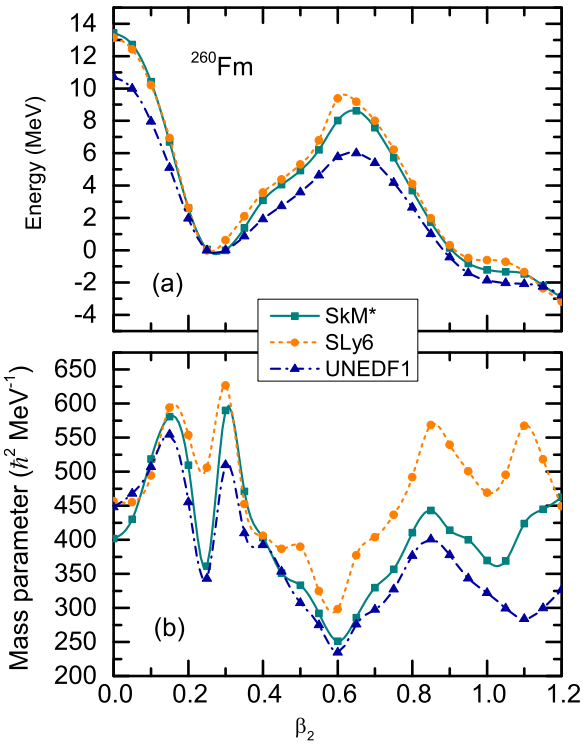

FIG. 2. (a) The calculated spontaneous fission barriers of ^{260}Fm with different Skyrme forces: SkM*, SLy6, and UNEDF1, respectively. (b) The calculated collective mass parameters of ^{260}Fm with the three Skyrme forces.

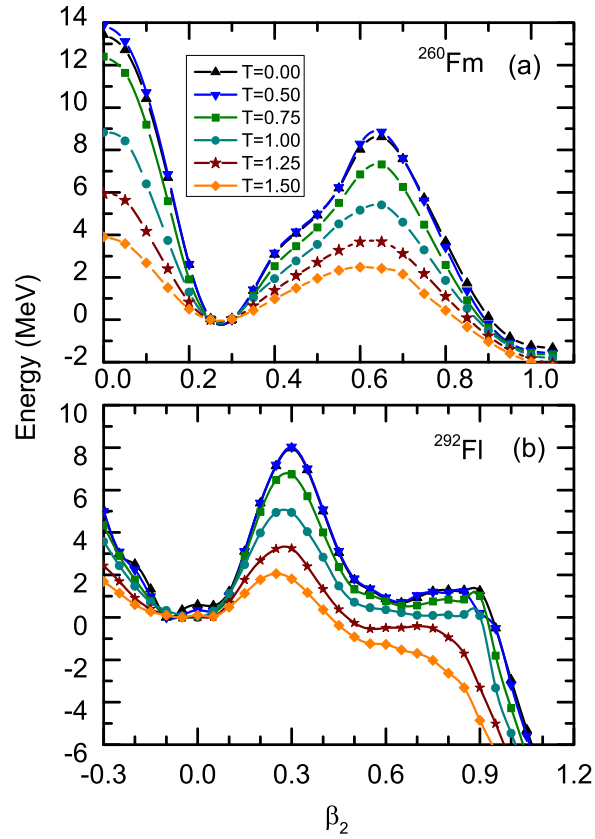

FIG. 3. The calculated temperature dependent fission barriers as a function of quadrupole deformation β_2, (a) for ^{260}Fm and (b) for ^{292}114. In ^{292}114, the reflection asymmetric deformation has been taken into account.

B. Temperature dependent fission barriers and mass parameters

We studied the temperature dependence of fission barriers of selected nuclei, ^{240}Pu, ^{260}Fm, ^{278}Cn, and ^{292}Fl. Our results obtained with FT-HF+BCS are very close to the earlier FT-HFB results. For example, thermal fission barriers of ^{240}Pu has been given in Ref. [54]; ^{278}Cn and ^{292}Fl have been shown in Ref. [19]. Figure 3 shows the temperature dependent fission barriers of ^{260}Fm and ^{292}Fl. Previously, the asymmetric fission mode of ^{292}Fl has not been included [19]. In this work, we do see the asymmetric fission mode is important for ^{292}Fl and the second barrier is almost gone. We see the fission barriers are almost unchanged at low temperatures and even slightly increased at $T = 0.5$ MeV when the pairing is significantly reduced. This has also been discussed in several earlier works [19,54]. After $T = 0.5$, the fission barrier heights decrease with increasing temperatures, which can be described by a damping factor to describe the melting of shell effects [17]. It is known that microscopic damping factors change rapidly in various nuclei [17,23], which are beyond phenomenological descriptions.

In addition to fission barrier heights, the temperature dependent curvatures (or frequencies) around the equilibrium point and the saddle point are also important. In Fig. 4, the obtained potential frequencies of ^{260}Fm and ^{292}Fl are shown, which are estimated by Eq. (14). At temperatures below $T = 0.5$ MeV, the frequencies change very slowly. For ^{260}Fm, it can be seen that the frequency ω_0 at the equilibrium point increases rapidly close to $T = 0.6$ MeV that is around the pairing phase transition temperature. ^{292}Fl is very special with a very small ω_0 that is associated with a very soft equilibrium deformation. Generally the frequencies ω_0 would be decreased as temperatures increased and compound nuclei would finally become spherical. The related collective energies E_n would be reduced with increasing temperatures. For both ^{260}Fm and ^{292}Fl, the frequencies ω_b at the saddle points also decrease as temperatures increase. Therefore the fission lifetimes can be enhanced due to the decreasing frequencies ω_0 and ω_b according to the ImF formula at high temperatures. We see the temperature dependencies of frequencies are different in various nuclei. This again demonstrated that microscopic calculations of temperature dependent fission barriers are valuable.

Figure 5 shows the temperature dependent behaviors of mass parameters of ^{260}Fm and ^{292}Fl. We studied the temperature dependence of mass parameters of selected nuclei with the temperature dependent cranking approximation. Compared to fission barriers, the mass parameters at high temperatures are rather nonsmooth. At zero temperature, the mass parameters is smooth due to the existence of pairing correlations. At the temperature of $T = 0.75$ MeV, it is around the critical temperature for the pairing phase transition and the mass parameters are increased and become very much irregular. It is

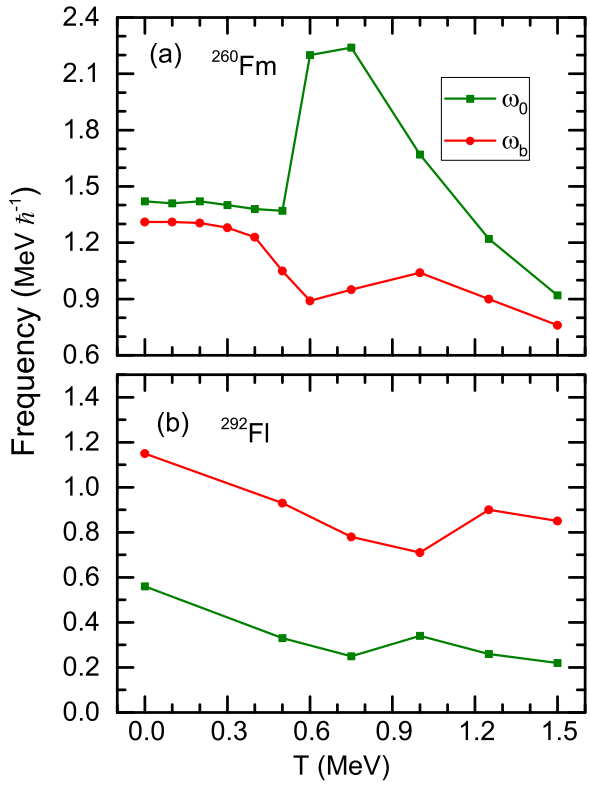

FIG. 4. The calculated potential curvatures (or frequencies) around the equilibrium point (ω_0) and the barrier saddle point (ω_b) as a function of temperature, (a) for ^{260}Fm and (b) for ^{292}Fl.

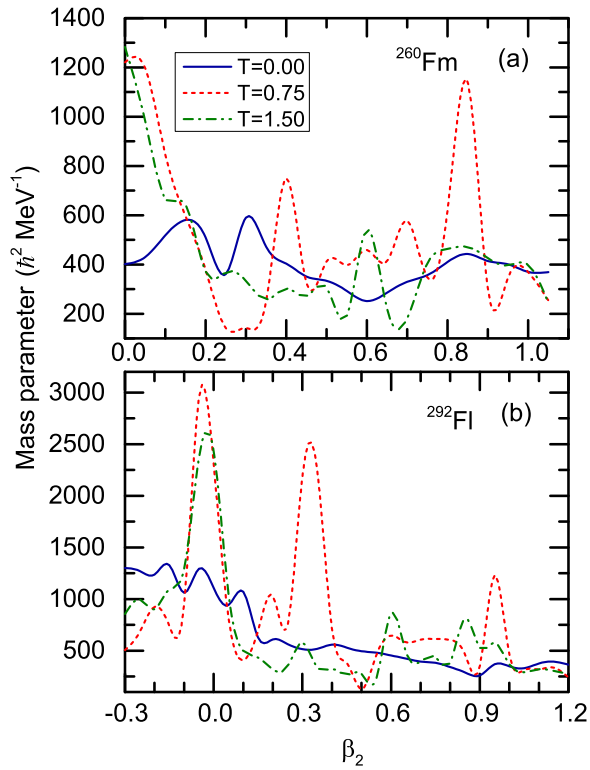

FIG. 5. (a) The calculated temperature-dependent mass parameters as a function of deformations, (a) for ^{260}Fm and (b) for ^{292}114.

TABLE II. The calculated fission lifetimes of ^{260}Fm and ^{240}Pu at low temperatures, based on the low-temperature ImF approach [see Eq. (10)]. The corresponding excitation energies are also given in MeV.

T (MeV)	^{260}Fm		^{240}Pu	
	E^*	T_f(s)	E^*	T_f(s)
0.1	0.001	1.50×10^{-3}	0.002	2.55×10^{10}
0.2	0.11	1.59×10^{-6}	0.13	2.80×10^{-3}
0.3	0.83	3.67×10^{-10}	0.81	4.50×10^{-8}
0.4	2.67	1.94×10^{-12}	2.43	3.48×10^{-10}
0.5	5.67	7.87×10^{-14}	4.85	9.08×10^{-11}
0.6	8.63	3.48×10^{-15}	7.02	8.17×10^{-12}
0.75	10.91	2.07×10^{-16}	11.19	9.61×10^{-13}

known that the collective inertia mass is inversely proportional to the square of the pairing gap [56]. As the temperature increases from $T = 0$ to $T = 0.75$ MeV the pairing gap decreases and therefore the mass parameters must increase. At the high temperature of $T = 1.5$ MeV, the mass parameters are much reduced and large peaks fade away due to statistical effects. This behavior has also been shown in Ref. [29]. In both ^{260}Fm and ^{292}Fl, the mass parameters at spherical shapes increase significantly compared to other deformations.

C. Thermal fission rates from low to high temperatures

In Table II, we studied the temperature dependence of fission rates of ^{240}Pu and ^{260}Fm according to the low-temperature ImF formula Eq. (10), from $T = 0.1$ to 0.75 MeV. We can see that the calculated fission lifetimes decrease very rapidly with increasing temperatures. For example, the lifetime has been decreased by 3 orders in ^{260}Fm at an excitation energy of 100 keV (around the astrophysical temperature T_9). At an excitation energy around 5 MeV, its lifetime has been decreased by 10 orders, compared to the spontaneous fission lifetime. The calculated fission lifetimes of ^{240}Pu decrease even faster than that of ^{260}Fm. For ^{240}Pu, it has a very large ω_0 of 1.87 MeV and a very small ω_b of 0.54 MeV. Therefore it has a very low transition temperature, $T_c = \omega_b/2\pi = 0.08$ MeV, from quantum tunnelings to thermal decays. While the transition temperature in ^{260}Fm is $T_c = 0.21$ MeV that is much higher than that of ^{240}Pu. The low-temperature ImF formula maybe not suitable for ^{240}Pu due to a very low T_c. Besides, the fission rates should be modified considering the double-humped barrier in ^{240}Pu. There are a few measurements of thermal fission rates directly [57]. Actually it can be related to the fast neutron induced fission cross sections with abundant experimental data.

In Table III, we studied the temperature dependence of the fission rates of selected nuclei according to the high-temperature ImF formula, which is applicable for $T > T_c$. Generally, the calculated fission lifetimes at high temperatures decrease less rapidly compared to the low-temperature rates. The fission rates of ^{240}Pu and ^{260}Fm at low temperatures are also given. In ^{260}Fm, we indeed see a smooth connection (or crossover) between low and high temperature formulas

TABLE III. The fission lifetimes of selected nuclei are calculated according to the ImF formula at high temperatures [see Eq. (16)]. The excitation energy and lifetime are given in MeV and seconds, respectively.

T	^{260}Fm		^{240}Pu	
(MeV)	E^*	T_f(s)	E^*	T_f(s)
0.1			0.002	4.06×10^{16}
0.2			0.13	4.39×10^{-2}
0.3	0.83	1.90×10^{-9}	0.81	3.25×10^{-8}
0.4	2.67	4.90×10^{-12}	2.43	2.92×10^{-11}
0.5	5.67	9.03×10^{-14}	4.85	4.51×10^{-13}
0.6	8.63	1.85×10^{-15}	7.02	5.51×10^{-15}
0.75	10.91	1.11×10^{-17}	11.19	8.13×10^{-17}
1.0	23.92	4.72×10^{-19}	21.22	1.12×10^{-18}
1.25	38.38	6.01×10^{-20}	35.42	9.14×10^{-20}
1.5	58.80	2.29×10^{-20}	54.40	3.27×10^{-20}
T	^{278}Cn		^{292}Fl	
(MeV)	E^*	T_f(s)	E^*	T_f(s)
0.5	4.70	3.54×10^{-17}	5.82	1.01×10^{-13}
0.75	11.25	3.56×10^{-19}	14.1	1.25×10^{-16}
1.0	23.17	2.32×10^{-20}	24.27	1.66×10^{-18}
1.25	40.17		40.22	2.09×10^{-19}
1.5	62.34		69.01	7.33×10^{-20}

at temperatures slightly higher than T_c. For ^{240}Pu with $T_c = 0.08$ MeV, the high temperature ImF formula should be more reasonable from $T = 0.1$ MeV, compared to Table II. The low temperature ImF formula underestimates the fission lifetimes of ^{240}Pu at low temperatures and overestimate fission lifetimes at high temperatures, compared to the high temperature ImF formula.

We see the fission lifetime of ^{278}Cn is smaller than that of ^{292}Fl at high excitation energies by 2 orders. While such a difference is about 9 orders at zero temperature in Table I. The differences in fission lifetimes of different nuclei decrease with increasing temperatures as quantum effects fad away. At $T = 1.25$ MeV, the fission barrier of ^{278}Cn is almost gone in contrast to ^{292}Fl. The frequency ω_0 in ^{292}Fl is small that can enhance thermal fission lifetimes. At $T = 1.0$ and 1.5 MeV, its microscopic neutron emission lifetimes [18] are 1.8×10^{-19} and 1.7×10^{-20} s, which are much smaller than its corresponding fission lifetimes of 1.67×10^{-18} and 7.3×10^{-20} s. This leads to considerable survival probabilities of ^{292}Fl at high excitations by microscopic calculations, which are 90% at $T = 1.0$ MeV and 81% at $T = 1.5$ MeV, respectively.

Figure 6 displays the thermal fission lifetimes of ^{260}Fm from low to high temperatures obtained by different approaches with the same microscopic inputs. Generally the fission lifetimes decease very rapidly at low temperatures and decrease slowly at high temperatures. We see the fission lifetimes by ImF and Kramers formulas are close at high temperatures. At low temperatures, the Kramers formula overestimates the fission lifetimes. The Boltzmann fission lifetimes are close to the ImF results at low temperatures. The fission lifetimes are mainly determined by the barrier heights in the exponential function

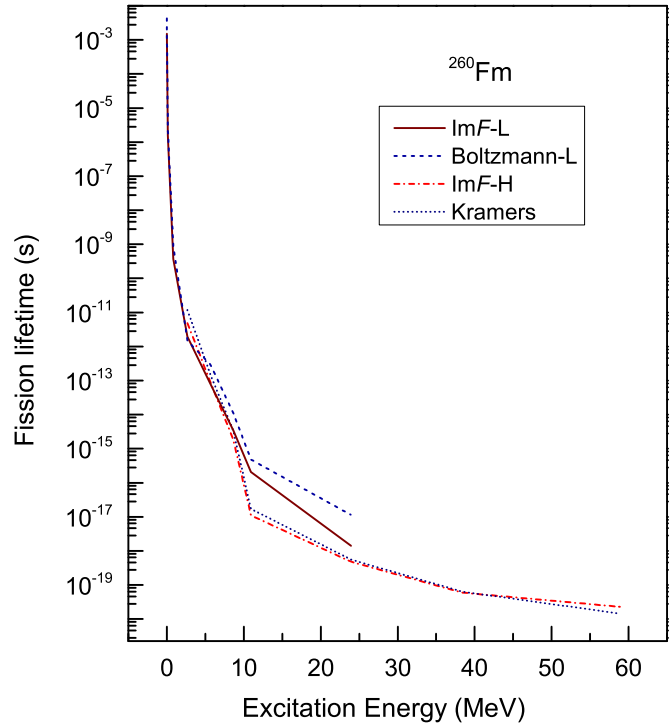

FIG. 6. The calculated thermal fission lifetimes of ^{260}Fm as a function of excitation energies by different formulas, in which 'ImF-L' denotes the low-temperature ImF formula Eq. (10), 'ImF-H' denotes the high-temperature ImF formula Eq. (16), 'Boltzmann-L' denotes the low-temperature Boltzmann thermal fission formula Eq. (9), 'Kramers' denotes the Kramers fission formula Eq. (17).

at high temperatures. Basically the low and high temperature ImF formulas are consistent although they have different temperature regimes of applicability regarding the transition temperature T_c. The two calculations have comparable results between $T = 0.3$ to 0.6 MeV, indicating a smooth transition from quantum tunneling to thermal decays. After $T = 0.6$ MeV, the above-barrier fission is important and the low-temperature formula overestimates the fission lifetimes. Based on results of ^{260}Fm, we see the low-temperature formula can be applied to temperatures that are slightly higher than T_c. In realistic calculations, the crossover of low and high temperature ImF formulas depends on not only T_c (or ω_b) but also the temperature dependent ω_0 and barrier heights. At temperatures higher than $T = 1.5$ MeV, the barriers and quantum effects are almost disappeared and the microscopic calculations would be questionable.

IV. SUMMARY

In summary, we studied the thermal fission rates with microscopic calculated temperature dependent fission barriers and mass parameters. The fission lifetime calculations are based on the imaginary free energy method from low to high temperatures in a consistent picture.

In Kramers and ImF methods, the fission barriers are given in terms of free energies which are naturally temperature

dependent. Our calculations involve only the effective Skyrme forces and pairing interactions without free parameters. We discussed the temperature dependent behaviors of fission barriers and mass parameters, which change rapidly in various nuclei and are beyond phenomenological descriptions. Therefore calculations of thermal fission rates with microscopic inputs are very necessary. With the previous microscopic neutron emission rates, we obtained considerable survival probabilities of ^{292}Fl at high excitations. We also emphasized the role of potential curvatures ω_0 and ω_b in the ImF formula. The curvatures are slowly decreasing from microscopic calculations at high temperatures and can enhance fission lifetimes. As a complementary, the spontaneous fission rates have also been studied. Our studies can be very useful for microscopic understandings of induced fission in reactors and the astrophysical r-process, and survival probabilities of compound superheavy nuclei. We noticed that large uncertainties still exist towards fully microscopic descriptions of thermal fission rates. In the future, it is worth to study both thermal fission rates and fragment distributions by semiclassical methods with microscopic inputs in multidimensional spaces.

ACKNOWLEDGMENTS

Discussions with W. Nazarewicz, P. Ring, J. Sadhukhan, N. Schunck, and F. R. Xu are gratefully acknowledged. This work was supported by the Research Fund for the Doctoral Program of Higher Education of China (Grant No. 20130001110001), and the National Natural Science Foundation of China under Grants No. 11375016, 11522538, 11235001.

[1] W. Younes and D. Gogny, AIP Conf. Proc. **1005**, 194 (2008).
[2] N. Schunck and L. M. Robledo, arXiv:1511.07517v2.
[3] A. Baran, J. A. Sheikh, J. Dobaczewski, W. Nazarewicz, and A. Staszczak, Phys. Rev. C **84**, 054321 (2011).
[4] P.-G. Reinhard and K. Goeke, Rep. Prog. Phys. **50**, 1 (1987).
[5] N. Hinohara, K. Sato, T. Nakatsukasa, M. Matsuo, and K. Matsuyanagi, Phys. Rev. C **82**, 064313 (2010).
[6] M. Kortelainen, J. McDonnell, W. Nazarewicz, P.-G. Reinhard, J. Sarich, N. Schunck, M. V. Stoitsov, and S. M. Wild, Phys. Rev. C **85**, 024304 (2012).
[7] J. Sadhukhan, K. Mazurek, A. Baran, J. Dobaczewski, W. Nazarewicz, and J. A. Sheikh, Phys. Rev. C **88**, 064314 (2013).
[8] A. Staszczak, A. Baran, J. Dobaczewski, and W. Nazarewicz, Phys. Rev. C **80**, 014309 (2009).
[9] B. N. Lu, J. Zhao, E. G. Zhao, and S. G. Zhou, Phys. Rev. C **89**, 014323 (2014).
[10] H. J. Krappe and K. Pomorski, *Theory of Nuclear Fission* (Springer-Verlag, Berlin, 2012).
[11] J. S. Langer, Ann. Phys. (NY) **41**, 108 (1967).
[12] I. Affleck, Phys. Rev. Lett. **46**, 388 (1981).
[13] K. Hagino, N. Takigawa, and M. Abe, Phys. Rev. C **53**, 1840 (1996).
[14] M. Kryvohuz, J. Chem. Phys. **134**, 114103 (2011).
[15] A. L. Goodman, Nucl. Phys. A **352**, 30 (1981).
[16] J. L. Egido, L. M. Robledo, and V. Martin, Phys. Rev. Lett. **85**, 26 (2000).
[17] J. C. Pei, W. Nazarewicz, J. A. Sheikh, and A. K. Kerman, Phys. Rev. Lett. **102**, 192501 (2009).
[18] Y. Zhu and J. C. Pei, Phys. Rev. C **90**, 054316 (2014).
[19] J. C. Pei, W. Nazarewicz, J. A. Sheikh, and A. K. Kerman, Nucl. Phys. A **834**, 381c (2010).
[20] J. O. Newton, D. G. Popescu, and J. R. Leigh, Phys. Rev. C **42**, 1772 (1990).
[21] M. G. Itkis, Yu. Ts. Oganessian, and V. I. Zagrebaev, Phys. Rev. C **65**, 044602 (2002).
[22] C. J. Xia, B. X. Sun, E. G. Zhao, and S. G. Zhou, Sci. China Phys. Mech. Astron. **54**, 109 (2011).
[23] J. A. Sheikh, W. Nazarewicz, and J. C. Pei, Phys. Rev. C **80**, 011302(R) (2009).
[24] J. H. Hamilton, S. Hofmann, and Y. T. Oganessian, Annu. Rev. Nucl. Part. Sci. **63**, 383 (2013).
[25] W. Loveland, Eur. Phys. J. A **51**, 120 (2015).
[26] J. D. McDonnell, W. Nazarewicz, and J. A. Sheikh, AIP Conf. Proc. **1175**, 371 (2009).
[27] A. Baran, K. Pomorski, A. Lukasiak, and A. Sobiczewski, Nucl. Phys. A **361**, 83 (1981).
[28] A. Iwamoto and W. Greiner, Z. Phys. A **292**, 301 (1979).
[29] V. Martin and L. M. Robledo, Int. J. Mod. Phys. E **18**, 861 (2009).
[30] N. T. Maitra and E. J. Heller, Phys. Rev. A **54**, 4763 (1996).
[31] A. Bulgac, P. Magierski, K. J. Roche, and I. Stetcu, Phys. Rev. Lett. **116**, 122504 (2016).
[32] J. Sadhukhan, W. Nazarewicz, and N. Schunck, Phys. Rev. C **93**, 011304(R) (2016).
[33] P. Goddard, P. Stevenson, and A. Rios, Phys. Rev. C **93**, 014620 (2016).
[34] D. Regnier, N. Dubray, N. Schunck, and M. Verriere, Phys. Rev. C **93**, 054611 (2016).
[35] *Dynamical Tunneling: Theory and Experiment*, edited by S. Keshavamurthy and P. Schlagheck (CRC Press, Boca Raton, FL, 2011).
[36] J. Erler, K. Langanke, H. P. Loens, G. Martínez-Pinedo, and P.-G. Reinhard, Phys. Rev. C **85**, 025802 (2012).
[37] A. Staszczak, A. Baran, and W. Nazarewicz, Phys. Rev. C **87**, 024320 (2013).
[38] P.-G. Reinhard, computer code SKYAX (unpublished).
[39] J. Bartel, P. Quentin, M. Brack, C. Guet, and H.-B. Håkansson, Nucl. Phys. A **386**, 79 (1982).
[40] J. Dobaczewski, W. Nazarewicz, and M. V. Stoitsov, Eur. Phys. J. A **15**, 21 (2002).
[41] B. Buck, A. C. Merchant, and S. M. Perez, Phys. Rev. C **45**, 2247 (1992).
[42] A. Baran, M. Kowal, P.-G. Reinhard, L. M. Robledo, A. Staszczsk, and M. Warda, Nucl. Phys. A **944**, 442 (2015).
[43] J. Libert, M. Girod, and J.-P. Delaroche, Phys. Rev. C **60**, 054301 (1999).
[44] A. Baran and Z. Lojewski, Acta Phys. Pol. B **25**, 1231 (1994).
[45] U. Weiss, *Quantum Dissipative Systems* (World Scientific Publishing, Singapore, 2012).
[46] D. Waxman and A. J. Leggett, Phys. Rev. B **32**, 4450 (1985).
[47] K. H. Schmidt, Int. J. Mod. Phys. E **18**, 850 (2009).
[48] Y. Jia, L. Liu, and J. D. Bao, Chin. Phys. C **27**, 610 (2003) (in Chinese).

[49] T. Bürvenich, M. Bender, J. A. Maruhn, and P.-G. Reinhard, Phys. Rev. C **69**, 014307 (2004).
[50] J. Sadhukhan, J. Dobaczewski, W. Nazarewicz, J. A. Sheikh, and A. Baran, Phys. Rev. C **90**, 061304(R) (2014).
[51] E. Chabanat, P. Bonche, P. Haensel, J. Meyer, and R. Schaeffer, Nucl. Phys. A **635**, 231 (1998).
[52] M. Bender, K. Rutz, P.-G. Reinhard, and J. A. Maruhn, Eur. Phys. J. A **7**, 467 (2000).
[53] S. A. Giuliani, L. M. Robledo, and R. Rodríguez-Guzmán, Phys. Rev. C **90**, 054311 (2014).
[54] N. Schunck, D. Duke, and H. Carr, Phys. Rev. C **91**, 034327 (2015).
[55] http://www.nndc.bnl.gov/.
[56] G. Bertsch and H. Flocard, Phys. Rev. C **43**, 2200 (1991).
[57] D. Jacquet and M. Morjean, Prog. Part. Nucl. Phys. **63**, 155 (2009).